

04

# Oscillatory current behavior in a pulsed gas discharge in atmospheric-pressure helium

© V.S. Kurbanismailov<sup>1</sup>, G.B. Ragimkhanov<sup>1</sup>, D.V. Tereshonok<sup>2</sup>, Z.R. Khalikova<sup>1</sup>

<sup>1</sup> Dagestan State University, Makhachkala, Dagestan Republic, Russia

<sup>2</sup> Joint Institute for High Temperatures, Russian Academy of Sciences, Moscow, Russia

E-mail: gb-r@mail.ru

Received July 3, 2025

Revised July 17, 2025

Accepted July 21, 2025

This paper presents the results of an experimental study of a pulsed gas discharge in helium at pressures of 1–3 atm in a plane-parallel gap with a mesh cathode and preliminary ultraviolet preionization. At an electron density of about  $10^8 \text{ cm}^{-3}$ , the discharge was initiated at voltages ranging from 3 to 14 kV. Analysis of current oscillograms revealed two stable regimes: aperiodic and oscillatory, differing in amplitude and pulse duration. It is shown that within a certain range of parameters — initial voltage, ballast resistance, and gas pressure — the current oscillation period, when present, remains constant.

**Keywords:** pulsed gas discharge, helium, preionization, mesh cathode, oscillatory regime.

DOI: 10.61011/TPL.2025.11.62196.20429

The study of pulsed gas discharges retains both fundamental and applied relevance [1–10]. The results of such research find wide application in surface processing, plasma aerodynamics, plasma-assisted combustion, plasma medicine, and other technological processes.

Despite the progress in experimental diagnostics, it is a highly complex task to obtain a complete spatiotemporal pattern of plasma evolution within the entire discharge gap. The influence of preionization on the dynamics of discharge development is of particular interest.

Experimental data reveal that, depending on external conditions, a discharge with gas preionization may proceed in homogeneous volume, volume with cathode spots, contracted, and high-current diffuse regimes [11,12]. As was demonstrated in [11–18], the initial stage of evolution of a pulsed volume discharge in inert gases with preionization is the formation of ionization waves; this conclusion was verified by both numerical modeling and high-speed imaging of the early stages of the discharge process.

However, it should be noted that the discharge characteristics are affected not only by the applied field, pressure, gas, and pre-ionization electron density, but also by the parameters of an *RLC*-circuit, where one may introduce the effective values of resistance *R*, inductance *L*, and capacitance *C* [19,20].

In the present study, we report the results of examination of oscilloscope records of current and integral glow patterns of a plane-parallel discharge in helium at pressures  $p = 1\text{--}3 \text{ atm}$  and voltages varying within a wide range of  $U_0 = 3\text{--}14 \text{ kV}$ .

The schematic diagram of the setup is shown in Fig. 1. Discharge gap *S* was a system of two electrodes: a top planar anode made of stainless steel with radius  $r_0 = 2 \text{ cm}$  and a bottom mesh cathode located parallel to the anode.

The interelectrode distance was  $d = 1 \text{ cm}$ . Helium with a chemical purity of at least 99.99 % was the working gas.

To establish the needed vacuum, the chamber was evacuated using a Welch CDK 240 (ILMVAC) turbomolecular pump that provided a maximum residual pressure on the order of  $5 \cdot 10^{-5} \text{ Pa}$ .

Preionization was performed by a spark discharge positioned behind a mesh anode. The time delay between the arrival of a high-voltage pulse and the switching-on of illumination was 100–150 ns, and the light pulse duration was on the order of 600 ns. An electron density on the order

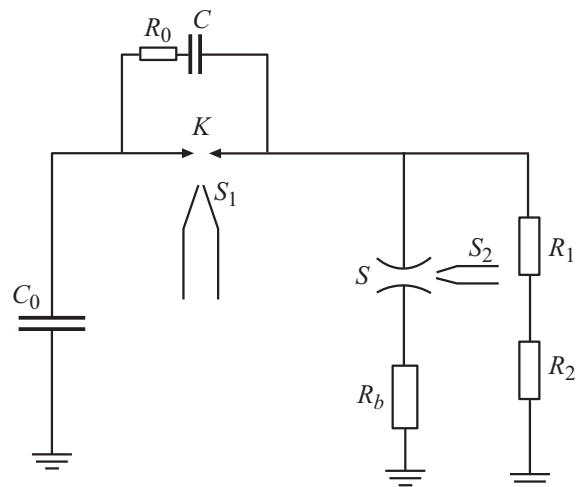


**Figure 1.** Schematic diagram of the setup:  $C_0$  — discharge capacitance,  $R_b$  — ballast resistance,  $K$  — switch,  $S_1$  — source of preionization of the gas medium of the switch,  $S$  — main discharge gap, and  $S_2$  — source of preionization of the main discharge gap ( $R_0 = 300 \Omega$ ,  $R_1 = 21.3 \text{ k}\Omega$ ,  $R_2 = 765 \Omega$ ,  $C = 4 \text{ nF}$ ,  $C_0 = 15 \text{ nF}$ ).

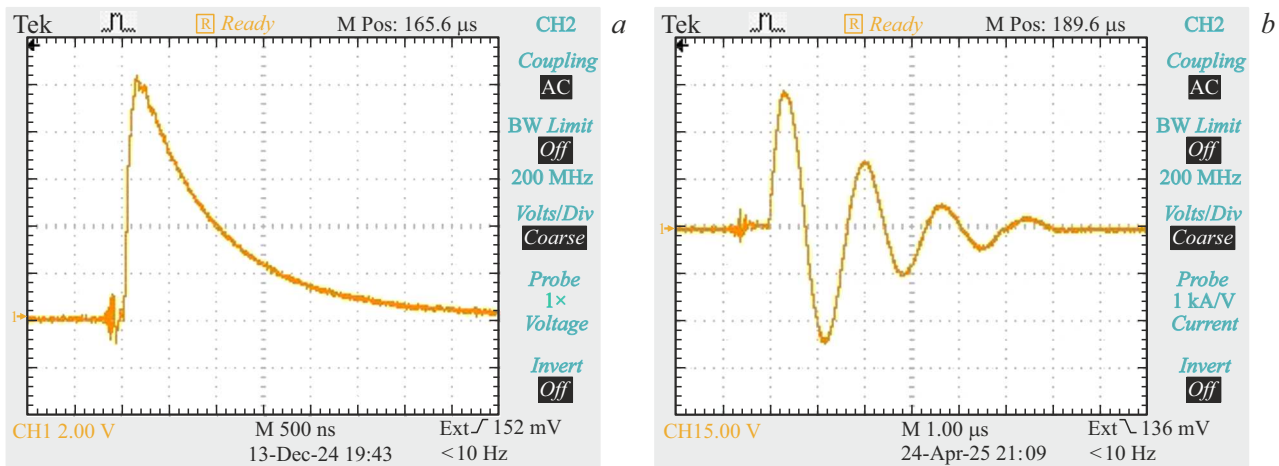


**Figure 2.** Characteristic oscilloscope records of the discharge current in aperiodic (a) and oscillatory (b) regimes at  $U_0 = 8$  kV,  $R_b = 52 \Omega$ .

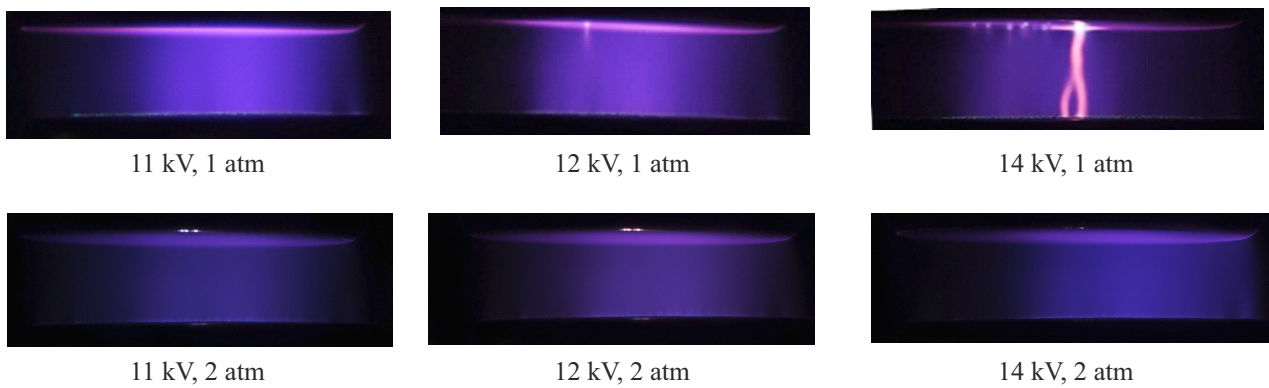


**Figure 3.** Integral patterns of discharge glow (oscillatory regime):  $R_b = 52 \Omega$ .

of  $10^8 \text{ cm}^{-3}$  was achieved with an energy input into the auxiliary discharge (source of UV radiation) of 0.3–0.4 J.

To examine the influence of voltage  $U_0$  at the discharge capacitance and gas pressure  $p$  on the discharge characteristics, integral glow patterns were recorded using a Sony Alpha A7 III (ILCE-7M3B) mirrorless digital camera with a lens with a focal length of 85 mm.

The electrical characteristics of the discharge (voltage and current) were recorded using an ohmic voltage divider and a low-inductance shunt. Signals were visualized by a Tektronix TDS2024C four-channel digital storage oscilloscope with a bandwidth of 200 MHz. The error of current amplitude measurement did not exceed 3%. High-voltage pulses were supplied from a pulse generator that could adjust the amplitude at  $C_0$  from 3 to 14 kV. The time of voltage rise to its peak value was up to 10 ns.

The studies of electrical and integral glow patterns were carried out in two discharge formation regimes established with ballast resistances  $R_b = 2$  and  $52 \Omega$  connected to the discharge gap. Two fundamentally different discharge regimes (aperiodic and oscillatory) corresponding to different distances  $S_1$  between the electrodes in the switch were identified.

Figure 2 shows typical oscilloscope records of the discharge current at voltage  $U_0 = 8$  kV. It can be seen from the oscilloscope records that, under otherwise equal conditions, the current flow regime changes from aperiodic (Fig. 2, a) to oscillatory (Fig. 2, b) as the interelectrode gap width in the switch exceeds 2 mm.

With ballast resistance  $R_b = 52 \Omega$ , the amplitude value of current in the oscillatory regime is higher than in the aperiodic one; at lower resistances (e.g.,  $R_b = 2 \Omega$ ), the opposite is true: the current amplitude in the aperiodic regime is higher. In the oscillatory regime (Fig. 2, b), the period of current oscillations is  $T \approx 1.7 \mu\text{s}$  and is virtually independent of  $U_0$  and  $p$ . In addition, the discharge duration in the oscillatory regime increases with an increase in  $U_0$  and falls within the range of 5–7  $\mu\text{s}$  in the examined field interval.

Figure 3 presents the integral discharge glow patterns in the oscillatory current regime for  $R_b = 52 \Omega$  at different voltages and pressures ranging from 1 to 3 atm. In contrast to the aperiodic regime, the oscillatory one (at voltages through to 11 kV) allows one to form an extremely uniform volume discharge without pronounced diffuse channels and luminous spots on the electrodes (Fig. 3). A further

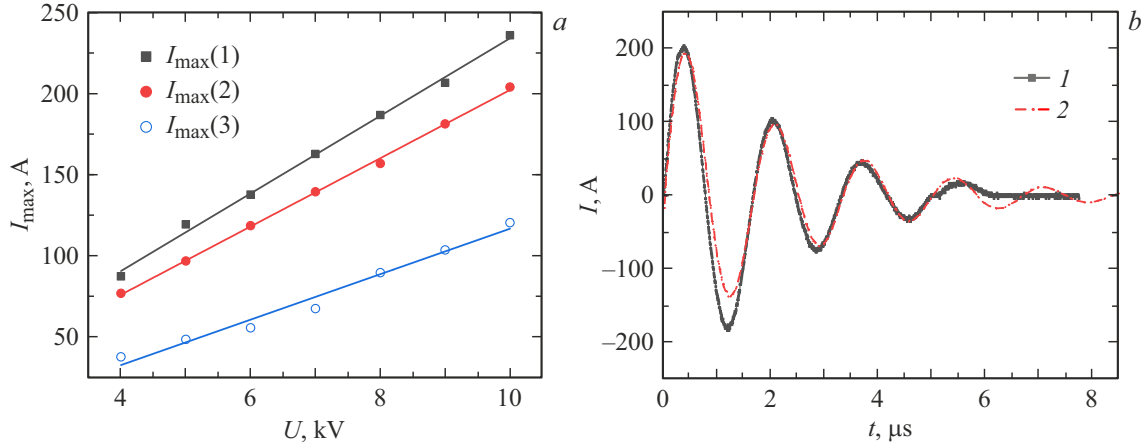


**Figure 4.** *a* — amplitude values of the discharge current in the oscillatory regime at pressure  $p = 1$  atm and ballast resistance  $R_b = 52 \Omega$  for the first three maxima in Fig. 2, *b*; *b* — characteristic oscilloscope records of the discharge current in the oscillatory regime:  $U_0 = 8$  kV,  $R_b = 52 \Omega$  (*I* — experiment, 2 — calculation based on Eq. (1)).

intensification of the applied field leads to the emergence of explosive emission plumes on the solid electrode, which grow in number with an increase in  $U_0$ . At voltage  $U_0 = 14$  kV, integral patterns reveal the formation of a spark channel.

It can be seen from Fig. 3 that the brightness of the plasma column decreases with an increase in gas pressure, but the discharge also becomes more uniform. In addition, the current amplitude decreases and the discharge pulse duration increases.

Figure 4, *a* shows the amplitude values of current  $I$  recorded for the first three maxima in the oscillatory regime.

The oscillatory nature of current with polarity reversal (Fig. 2, *b*) makes it possible to introduce an effective inductance and substitute the actual circuit with an equivalent one in the form of an  $RLC$ -circuit, where  $R_d$ ,  $L_d$ , and  $C_d$  are the resistance, inductance, and capacitance of the discharge gap.

Let us write the Kirchhoff equations for the  $R_d L_d C_d$ -circuit:

$$L_d \frac{dI}{dt} + R_d I + \frac{1}{C_d} \int I dt = 0 \Rightarrow \frac{d^2 I}{dt^2} + 2\delta \frac{dI}{dt} + \omega_0^2 I = 0, \quad (1)$$

$$\delta = \frac{R_d}{2L_d}, \quad \omega_0 = \frac{1}{\sqrt{L_d C_d}}.$$

The solution of (1) is  $I(t) = I_0 e^{-\delta t} \sin(\omega t + \varphi)$ , where  $\omega = \sqrt{\omega_0^2 - \delta^2} = \frac{2\pi}{T}$ . Here,  $\varphi = 0$  under the condition that  $I(t = 0) = 0$ . Determining the attenuation coefficient as the ratio of amplitudes of the first and third current maxima from Fig. 4, *b*  $\delta = \frac{\ln(I_0/I(T))}{T} = \frac{\ln(2.3 \pm 0.4)}{T}$ , we obtain equality

$$\omega = \sqrt{\omega_0^2 - \delta^2} = \sqrt{\frac{1}{L_d C_d} - \frac{R_d^2}{4L_d^2}}$$

$$= \sqrt{\frac{1}{L_d C_d} - \left( \frac{\ln(I_0/I(T))}{T} \right)^2} = \frac{2\pi}{T}, \quad (2)$$

which provides the following expression for product  $L_d C_d$ :

$$L_d C_d = \frac{T^2}{4\pi^2 + (\ln(I_0/I(T)))^2} \approx \left( \frac{T}{2\pi} \right)^2$$

$$\Rightarrow \omega \approx \omega_0 = \frac{1}{\sqrt{L_d C_d}}. \quad (3)$$

In accordance with (3), the observed period of oscillations (if they appear) depends, at least within the studied range of parameters, just on product  $C_d L_d$  of the capacitance and inductance of the equivalent circuit of the discharge gap. Figure 4, *b* presents an example comparison of experimental oscilloscope records of current (Fig. 2, *b*) for  $U_0 = 8$  kV and  $R_b = 52 \Omega$  with calculated values derived from the solution of Eq. (1) with an experimentally determined cyclic frequency. A similar match is observed for other combinations of  $U_0$ ,  $p$ , and the interelectrode distance in the switch in the oscillatory regime.

Thus, two fundamentally different regimes of discharge in helium in the examined circuit were identified. With a small interelectrode gap  $S_1$  of the switch, the discharge current pulse has an aperiodic shape. As  $S_1$  increases, it assumes a distinct oscillatory nature with an almost constant period  $T \approx 1.7 \mu$ s that does not depend on voltage and pressure. The oscillatory regime produces a much more uniform glow without bright cathode (anode) spots at voltages up to 11 kV. The obtained results are important in the context of optimization of plasma radiation sources and design of gas discharge systems in media with elevated pressures of several atmospheres, where diffuse discharge regimes stable over time scales of  $1 \mu$ s or more are required.

## Funding

This study was supported financially by the Russian Science Foundation (project No. 25-22-20090).

## Conflict of interest

The authors declare that they have no conflict of interest.

## References

- [1] M. Erofeev, V. Ripenko, M. Shulepov, V. Tarasenko, *Eur. Phys. J. D*, **71**, 117 (2017). DOI: 10.1140/epjd/e2017-70636-6
- [2] S.M. Starikovskaia, *J. Phys. D*, **47**, 353001 (2014). DOI: 10.1088/0022-3727/47/35/353001
- [3] N.A. Popov, *Plasma Sources Sci. Technol.*, **20**, 045002 (2011). DOI: 10.1088/0963-0252/20/4/045002
- [4] N.L. Aleksandrov, S.V. Kindysheva, I.N. Kosarev, S.M. Starikovskaia, A.Yu. Starikovskii, *Proc. Combust. Inst.*, **32**, 205 (2009). DOI: 10.1016/j.proci.2008.06.124
- [5] D.V. Tereshonok, N.Yu. Babaeva, G.V. Naidis, V.A. Panov, B.M. Smirnov, E.E. Son, *Plasma Sources Sci. Technol.*, **27** (4), 045005 (2018). DOI: 10.1088/1361-6595/aab6d4
- [6] Yu.D. Korolev, G.A. Mesyats, *Fizika impul'snogo proboya gazov* (Nauka, M., 1991) (in Russian).
- [7] V.F. Tarasenko, E.Kh. Baksht, A.G. Burachenko, M.I. Lomaev, D.A. Sorokin, Yu.V. Shut'ko, *Tech. Phys. Lett.*, **36** (4), 375 (2010). DOI: 10.1134/S1063785010040255.
- [8] V.V. Osipov, *Phys. Usp.*, **43** (3), 221 (2000). DOI: 10.1070/pu2000v043n03ABEH000602.
- [9] V.F. Tarasenko, S.I. Yakovlenko, *Phys. Usp.*, **47** (9), 887 (2004). DOI: 10.1070/PU2004v047n09ABEH001790.
- [10] L.P. Babich, E.I. Bochkov, I.M. Kutsyk, *JETP Lett.*, **99** (7), 386 (2014). DOI: 10.1134/S0021364014070029.
- [11] V.S. Kurbanismailov, O.A. Omarov, G.B. Ragimkhanov, D.V. Tereshonok, *Tech. Phys. Lett.*, **43** (9), 853 (2017). DOI: 10.1134/S1063785017090206.
- [12] V.S. Kurbanismailov, O.A. Omarov, *Teplofiz. Vys. Temp.*, **33** (3), 346 (1995) (in Russian).
- [13] V.S. Kurbanismailov, D.V. Tereshonok, G.B. Ragimkhanov, Z.R. Khalikova, *Tech. Phys. Lett.*, **48** (3), 41 (2022). DOI: 10.21883/TPL.2022.03.53525.19067.
- [14] N.Yu. Babaeva, G.V. Naidis, *J. Phys. D*, **54** (22), 223002 (2021). DOI: 10.1088/1361-6463/abe9e0
- [15] A. Sobota, F. Manders, E.M. van Veldhuizen, J. van Dijk, M. Haverlag, *IEEE Trans. Plasma Sci.*, **38** (9), 2289 (2010). DOI: 10.1109/TPS.2010.2056934
- [16] V.S. Kurbanismailov, O.A. Omarov, G.B. Ragimkhanov, D.V. Tereshonok, *Europhys. Lett.*, **123** (4), 45001 (2018). DOI: 10.1209/0295-5075/123/45001
- [17] B.-D. Huang, Ch. Zhang, W. Zhu, X. Lu, T. Shao, *High Voltage*, **6** (4), 665 (2021). DOI: 10.1049/hve2.12067
- [18] D.V. Tereshonok, N.Y. Babaeva, G.V. Naidis, A.G. Abramov, A.V. Ugryumov, *IEEE Trans. Plasma Sci.*, **50** (3), 580 (2022). DOI: 10.1109/TPS.2022.3148545
- [19] A. Sobota, O. Guaitella, A. Rousseau, *Plasma Sources Sci. Technol.*, **23**, 025016 (2014). DOI: 10.1088/0963-0252/23/2/025016
- [20] T.H. Chung, *IEEE Trans. Plasma Sci.*, **42** (12), 3656 (2014). DOI: 10.1109/TPS.2014.2364056

*Translated by D.Safin*